

# Apparent fractal dimensions in the HMF model

Luca Sguanci<sup>1</sup>, Dieter H. E. Gross<sup>2</sup> and Stefano Ruffo<sup>3</sup>

1. *Dipartimento di Energetica “S. Stecco”, Università di Firenze, Via S.Marta, 3 I-50139, Firenze, Italy*

2. *Hahn Meitner Institute, Bereich SF5 Glienicker Str.100, D14109 Berlin, Germany*

3. *Dipartimento di Energetica “S. Stecco” and CSDC, Università di Firenze, INFN and INFN, Via S.Marta, 3 I-50139, Firenze, Italy*

---

## Abstract

We show that recent observations of fractal dimensions in the  $\mu$ -space of  $N$ -body Hamiltonian systems with long-range interactions are due to finite  $N$  and finite resolution effects. We provide strong numerical evidence that, in the continuum (Vlasov) limit, a set which initially is not a fractal (e.g. a line in 2D) remains such for all finite times. We perform this analysis for the Hamiltonian Mean Field (HMF) model, which describes the motion of a system of  $N$  fully coupled rotors. The analysis can be indirectly confirmed by studying the evolution of a large set of initial points for the Chirikov standard map.

*Key words:* Hamiltonian dynamics, Vlasov equation, Fractal dimensions.

*PACS numbers:*

05.45.-a Nonlinear dynamics and nonlinear dynamical systems,

05.45.Df Fractals

52.65.Ff Fokker-Planck and Vlasov equation.

---

It has been recently claimed [1,2] that structures characterized by a non integer fractal dimension [3] form spontaneously in the  $\mu$ -space of some  $N$ -body Hamiltonian systems, even when starting from a set of initial conditions (points in  $\mu$ -space) that does not show any fractality.

<sup>1</sup> E-mail: luke@dma.unifi.it

<sup>2</sup> E-mail: gross@hmi.de

<sup>3</sup> E-mail: ruffo@avanzi.de.unifi.it

The model analysed in Ref. [1] is the one-dimensional self-gravitating system [4] and the initial condition is a *line* in  $\mu$ -space, corresponding to a vanishing virial ratio (zero velocity for all mass sheets). The model studied in Ref. [2] describes the motion of a fully coupled system of  $N$  rotors and goes under the name of Hamiltonian Mean Field (HMF) model [5]; the initial condition is such that all rotors are fixed at some given angle (conventionally zero) and angular velocities are uniformly spread in an interval, symmetric around zero.

There is a strong analogy between the two results since: *i*) both models possess a continuum mean-field limit ( $N \rightarrow \infty$  at fixed volume) for which the single particle distribution function (SPDF)  $f(q, p, t)$  evolves according to a Vlasov-Poisson system [6], *ii*) both initial states are *lines* in  $\mu$ -space when the continuum limit is taken.

In this short note we analyse the HMF model, considering the same initial state as the one studied in Ref. [2]. We give compelling numerical evidence that, as the number of rotors grows and as the resolution increases, the collection of initial points lies on a set of dimension one in the  $\mu$ -space (which is two-dimensional for this model) at all finite times.

We will explain that this is a somewhat trivial consequence of the fact that the SPDF obeys a Vlasov equation in the mean-field limit. Moreover, we will show that *apparent fractal dimensions* can be indeed observed at low resolutions, justifying the observations of Ref. [2]. For comparison, we will show what happens for the standard Chirikov's map [7], which shares the symplectic property with the HMF model, for which we can push the analysis to a larger number of initial points.

The Hamiltonian of the HMF model is

$$H_{HMF} = \frac{1}{2} \sum_{j=1}^N p_j^2 + \frac{1}{2N} \sum_{j,k=1}^N [1 - \cos(q_j - q_k)], \quad (1)$$

where  $q_i \in [-\pi, \pi[$  is the position (angle) of the  $i$ -th particle on a circle and  $p_i$  the corresponding conjugate variable. This system can be seen as representing particles moving on a unit circle interacting via an infinite range attractive cosine potential, or as classical XY rotors with infinite range ferromagnetic couplings (for more details see Ref. [8]). The magnetization, defined as

$$\vec{M}(t) = (M_x, M_y) = \frac{1}{N} \sum_{j=1}^N (\cos q_j(t), \sin q_j(t)), \quad (2)$$

is the main observable that characterizes the dynamical and thermodynamic state of the system.

In the continuum limit, that is keeping the volume (here the interval  $[-\pi, \pi[$ ) and the energy per particle fixed as the number of particles  $N \rightarrow \infty$ , the dynamics governed

by Hamiltonian (1) is described by a Vlasov equation. Indeed, the state of the finite  $N$  system can be described by a single particle time-dependent distribution function

$$f_d(q, p, t) = \frac{1}{N} \sum_{j=1}^N \delta(q - q_j(t), p - p_j(t)) , \quad (3)$$

where  $\delta$  is the Dirac function. When  $N$  is large, it is natural to approximate the discrete density  $f_d$  by a continuous SPDF  $f(q, p, t)$ . Using this distribution, one can rewrite the two components of the magnetization  $M$  as

$$\overline{M}_x[f] \equiv \int f(q, p, t) \cos q \, dq dp \quad , \quad (4)$$

$$\overline{M}_y[f] \equiv \int f(q, p, t) \sin q \, dq dp \quad . \quad (5)$$

Within this approximation the potential that affects all the particles is

$$V(q)[f] = 1 - \overline{M}_x[f] \cos q - \overline{M}_y[f] \sin q \quad . \quad (6)$$

This potential enters the expression of the Vlasov equation

$$\frac{\partial f}{\partial t} + p \frac{\partial f}{\partial q} - \frac{dV}{dq}[f] \frac{\partial f}{\partial p} = 0 \quad , \quad (7)$$

which governs the spatio-temporal evolution of the SPDF  $f$ .

The initial condition considered in [2] is  $q_i = 0, \forall i$  and  $p_i$  random i.i.d. uniformly distributed in the interval  $[-\bar{p}, \bar{p}]$ . As usual, we call this class of initial conditions *water bags* (WB). The value of  $\bar{p}$  is chosen such that the energy per particle is  $U = H_{HMF}/N = 0.69$  and  $N = 10000$ , but these data will be varied in this paper. For such an energy this initial state is Vlasov unstable [9], and hence the SPDF evolves in time (see fig. 3 in Ref. [2]).

However, since initially the state is a *line* in the two-dimensional  $\mu$ -space  $(q, p)$ , it will remain a line for all finite times, although intricately stretched and folded. This is a trivial property related to the fact that Vlasov equation defines a *flow*  $\Phi_t$  for the particles (points  $\mathbf{x} = (q, p)$  in the  $\mu$ -space continuum)

$$\mathbf{x}(t) = \Phi_t(\mathbf{x}(0)) , \quad (8)$$

which is a diffeomorphism. Moreover, since the Jacobian  $J = \partial \mathbf{x}(t) / \partial \mathbf{x}(0)$  is a symplectic matrix, areas modify their shape but are conserved.

The reason why the set does not appear to be a line is due to the finite particle number in the simulation. The line is stretched and folded by the two main phase-space mechanisms: the formation of whorls around elliptic fixed points and of tendrils in the homoclinic tangle [10]. Moreover, local hyperbolicity in phase-space produces a dispersion of the initial points. As a consequence, the set of initial points, appears

by visual inspection, in the course of time, to be partly distributed along lines and partly dispersed onto the two-dimensional  $\mu$ -space (see again fig. 3 in Ref. [2] or fig. 2 in Ref. [1]) This is why the authors of Refs. [1,2] have used *fractal dimension* to characterize this set, more specifically box dimension [1] and correlation dimension [2].

The number of boxes  $N_b(\epsilon)$  of linear size  $\epsilon$  which cover the set of  $N = 10^6$  points at time  $t = 75$  when starting the HMF model in a WB initial condition at  $U = 0.69$  is shown as a function of resolution  $1/\epsilon$  in log-log scale in fig. 1. These data are not qualitatively different from the ones in fig. 3 of Ref. [1] and one might then fit the central part of them with the Ansatz  $N_b = \epsilon^{-D_0}$  (since the maximal box size which contains all the set is normalized to one), obtaining  $D_0 \sim 1.930 \pm 0.002$  and concluding that the set is a fractal, with dimension  $D_0$  close to two, but definitely distinct from two within numerical accuracy. This is a consequence of the set being a mixture of a set with one-dimensional features (the initial line) and two-dimensional ones caused by chaotic spread.

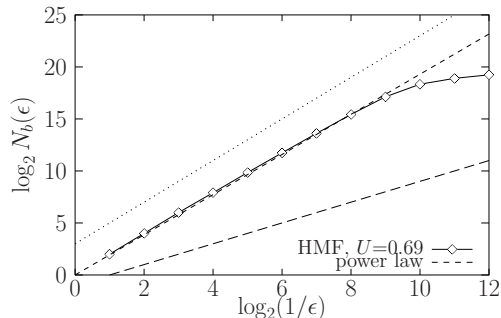


Fig. 1. Number of occupied boxes of linear size  $\epsilon$  versus resolution  $1/\epsilon$  in log-log scale for the HMF model in a WB initial condition with  $U = 0.69$  and  $N = 10^6$  ( $\diamond$ ). The short-dashed line superposed to the data is a power law fit with *apparent fractal dimension*  $D_0 \sim 1.93$ . The upper deviation from the power law is at  $1/\epsilon = 2^{10}$ , i.e. roughly when the number of boxes  $(1/\epsilon)^2$  is of the order of the number of points  $N$ . The dotted and long-dashed lines are the power laws with exponents 2 and 1, respectively.

However, as first remarked in Ref. [11] the slope of the curve in fig. 1 is not constant and depends on the resolution. It is already evident in this figure that, as the resolution increases ( $\epsilon \rightarrow 0$ ), the local slope tends to zero (on this scale most of the points are surrounded by very few neighbours). This is better shown in fig. 2a, where the discrete approximation of the local slope in logarithmic scale

$$s(\epsilon) = \frac{d \log_2 N_b(\epsilon)}{d \log_2(1/\epsilon)}, \quad (9)$$

is plotted as a function of  $\epsilon$  for the same set of points. Going from low to high resolution, all dimensions from 2 to 0 are covered continuously and smoothly. All are *apparent fractal dimensions* of a set which has indeed dimension 1. It might look strange that one does not observe any signal of dimension 1 at any resolution. This is due to the *inhomogeneity*, as shown in fig. 3, where one represents in black the occupied boxes at increasing resolutions. While at low resolutions all boxes are

occupied indicating a set of dimension 2, when the resolution increases, the set concentrates on a smaller set of boxes, but already at resolution  $1/\epsilon = 2^9$  one observes structures of dimension 1 (lines). However, their weight in the  $\mu$ -space is negligible and, as the resolution is increased even more, the fraction of the set made by spread points dominates and consequently dimension 0. A complete multifractal [3] analysis should be realized to highlight such inhomogeneities.

For comparison, we have performed a similar experiment for the Chirikov standard map [7]

$$p_{t+1}^i = p_t^i + q_t^i \tag{10}$$

$$q_{t+1}^i = q_t^i - K \sin(p_{t+1}^i) \pmod{2\pi} , \tag{11}$$

where the index  $t = 0, \dots$  denotes time and the index  $i = 1, \dots, NP$  the number of initial particles. Particles are put at  $t = 0$ , as above, at  $q = 0$  and with momentum uniformly spread in the interval  $[-\bar{p}, \bar{p}]$ . The phase space is closed by periodizing in  $2\pi$  both the  $q$  and the  $p$  directions and normalized in the unit square. The results of numerical experiments conducted above the chaos threshold, at  $K = 1.2$ , i.e. a parameter region with a *mixed* (chaotic and regular) phase space, are shown in fig. 2b (local slopes) and fig. 4 (occupied boxes in phase space at different resolutions). The behavior of all measured quantities is qualitatively the same as the one of the HMF model.

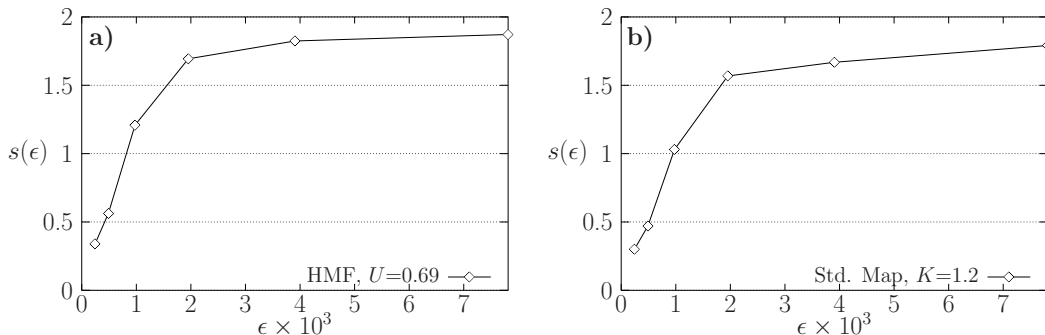


Fig. 2. Local slopes  $s(\epsilon)$  for resolutions ranging from  $1/\epsilon = 2^7$  up to  $2^{12}$ . In Figure **a)** we plot the results for the HMF model at  $t = 75$  with WB initial condition at  $U = 0.69$  and  $N = 10^6$ . Figure **b)** refers to the standard map at  $t = 160$  for  $K = 1.2$  and  $NP = 10^6$ .

Can one get from straight box-counting an indication of the presence of sets of dimension 1? To obtain this results it is enough to perform experiments at lower energies for the HMF model and at smaller values of parameter  $K$  in the standard map. By doing this, one decreases the fraction of phase space which is occupied by chaotic orbits and, hence, reduces particle dispersion. In fig. 5 we plot the local slopes for the HMF model at  $U = 0.1$  (fig. 5a) and at  $K = 0.2$  for the standard map (fig. 5b). In these cases, the local slope, and hence fractal dimension, shows an evident plateau at the value 1 as the resolution increases, before dropping to zero when the individual points of the set are detected. Let us remark that the number

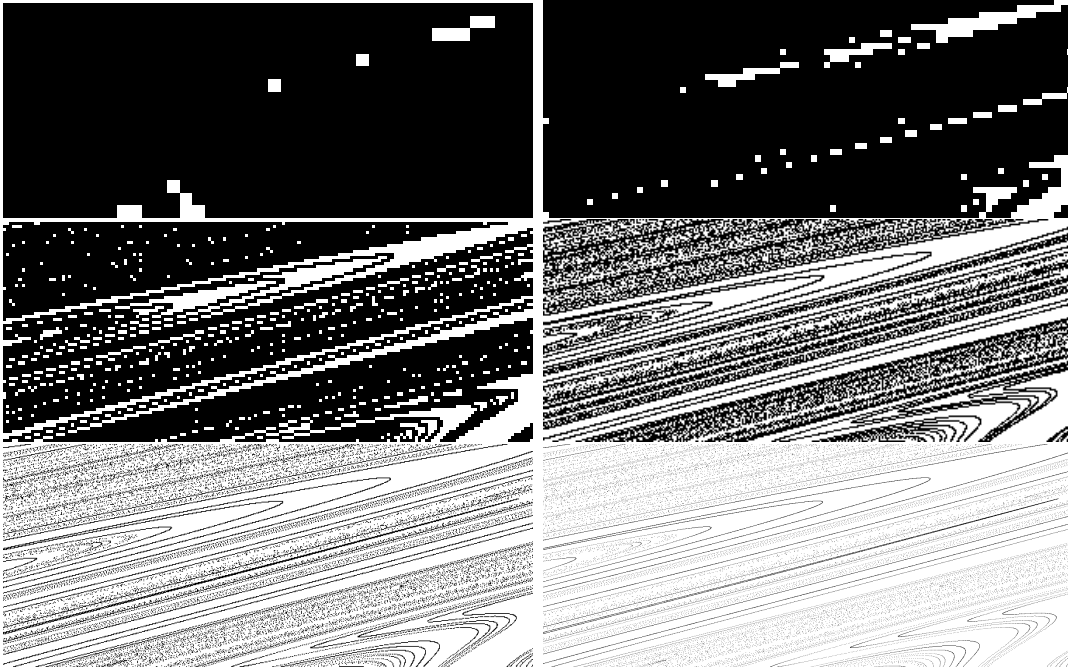


Fig. 3. HMF model. A set of  $N = 10^6$  points is, initially, uniformly distributed along the  $p$  axis between  $-\bar{p}$  and  $\bar{p}$ , such that  $U = \bar{p}^2/6 = 0.69$ . From left to right and from top to bottom we show a portion  $S = [0.33, 0.66[ \times [0.36, 0.50[$  of the  $\mu$ -space, where a box of given linear dimension  $\epsilon$  is colored black if at least one point of the initial condition is contained inside it at time  $t = 75$ . Resolution ranges from  $1/\epsilon = 2^7$  up to  $1/\epsilon = 2^{12}$ .

of particles is the same as before  $N = NP = 10^6$ . This is a strong evidence that the line remains a line during time evolution, as expected.

Having understood that the limited number of particles is crucial in determining the results, we show in fig. 6 and fig. 7 the dependence of the local slopes on the number of particles for both the HMF model and the standard map. In all cases,  $s$  is an increasing function of the number of particles, and, at fixed number of particles, as the resolution increases, the slope decreases. However, for a more chaotic phase space (fig. 6), i.e. HMF at  $U = 0.69$  and standard map at  $K = 1.2$ , the curves corresponding to the higher resolution show only a slight increase from zero slope and one cannot definitely conclude that, as the number of particle increases, they will tend to slope 1 (while those which converge, clearly point to dimension 2). On the contrary, for a less chaotic phase space (HMF at  $U = 0.1$  and standard map at  $K = 0.2$ ), the curves corresponding to the higher resolutions converge to slope (dimension) 1 as the number of particles increases, approximately to  $(1/\epsilon)^2$ .<sup>4</sup>

<sup>4</sup> For the standard map we have performed experiments for up to  $10^8$  particles. We have obtained a more evident levelling off of the slope as the number of particles increases and a convergence to 1 from above as the resolution subsequently increases. For the HMF model the convergence to 1 is followed by a further drop to smaller values at higher resolutions, as also shown in fig. 5a: this is again a finite  $N$  effect.

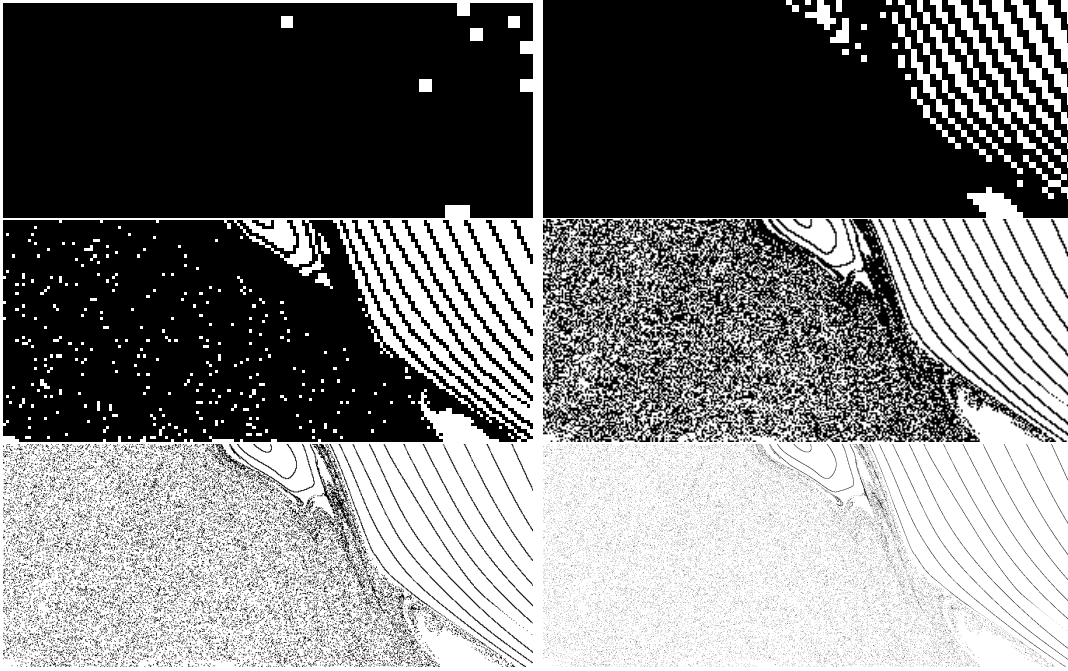


Fig. 4. Standard map at  $K = 1.2$ . A set of  $NP = 10^6$  particles is, initially, uniformly distributed along the  $p$  axis. From left to right and from top to bottom we show a portion  $S = [0, 0.33[ \times [0.86, 1.00[$  of the phase space, where a box of given linear dimension  $\epsilon$  is colored black if at least one particle of the initial condition is contained inside it at time  $t = 160$ . Resolution ranges from  $1/\epsilon = 2^7$  up to  $1/\epsilon = 2^{12}$ .

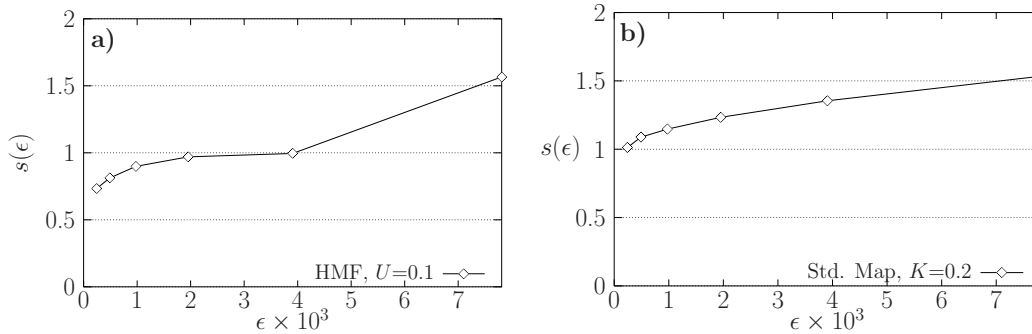


Fig. 5. This figure shows how the local slope changes for resolutions ranging from  $1/\epsilon = 2^8$  up to  $2^{12}$ . In Figure **a**) we plot the results at  $t = 500$  for the HMF model with WB initial condition corresponding to  $U = 0.1$  and a number of particles  $N = 10^6$ . Figure **b**) refers to the Standard Map at  $t = 160$  for  $K = 0.2$  and  $NP = 10^6$ . Again the “natural” slope  $s = 1$  is roughly at  $(1/\epsilon)^2 \sim N, NP$ .

We think that we have solved the puzzle of the existence of a fractal set generated in a finite time when starting with a one-dimensional set (a line) in the phase space of Hamiltonian systems. *The fractal is not there and is a feature of the resolution with which the set is observed.*

Of course this does not diminish the role played by fractal concepts in systems with long-range interactions. Certainly, when the initial set is already a fractal [12], it’s

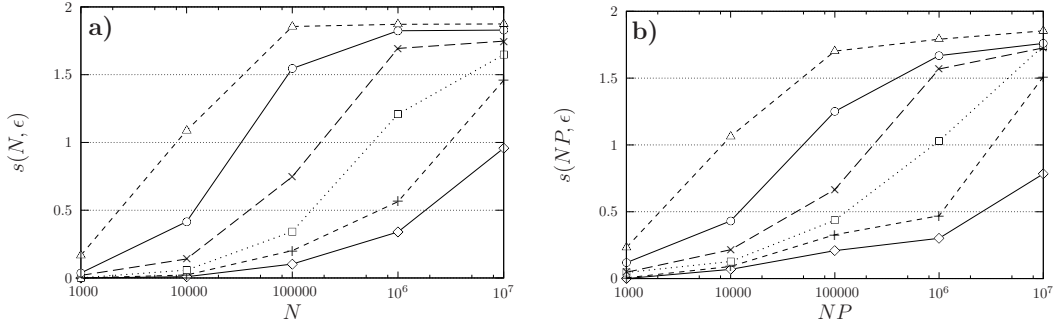


Fig. 6. Local slope as a function of the number of particles (ranging from  $10^3$  up to  $10^7$ ) for different values of the resolution  $1/\epsilon$ :  $2^7$  ( $\triangle$ );  $2^8$  ( $\circ$ );  $2^9$  ( $\times$ );  $2^{10}$  ( $\square$ );  $2^{11}$  ( $+$ );  $2^{12}$  ( $\diamond$ ). Figure **a**) shows the results for the HMF model at  $U = 0.69$  and Figure **b**) the corresponding results for the standard map at  $K = 1.2$ .

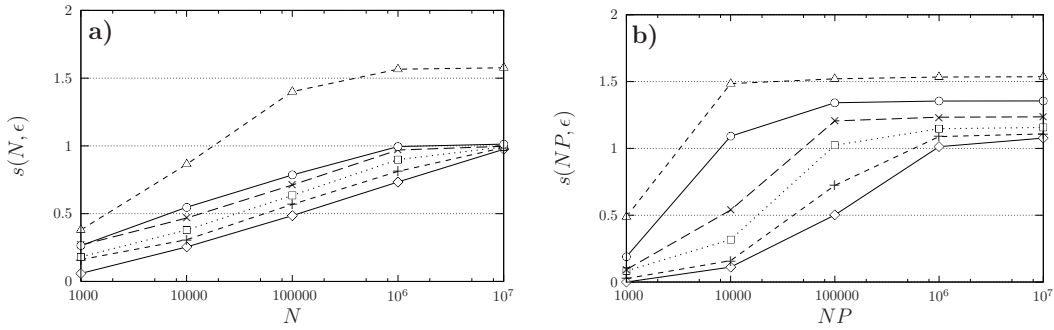


Fig. 7. Same as fig. 6 but for  $U = 0.1$  (HMF) **a**) and  $K = 0.2$  (standard map) **b**).

well possible that the set remains fractal during time evolution. Moreover, when studying evolving universe models, one effectively introduces dissipative terms in the equations of motion [12,13] and one can indeed observe fractal sets generated from non fractals. Another situation is the one of the advection of passive tracers [14] or vector fields [15], where one indeed can observe fractal sets in Hamiltonian phase spaces. This is due to the presence of non escaping orbits inside the mixing region, which form a zero measure fractal repeller [14] or, in the kinematic dynamo problem [15], to the concentration of the magnetic flux onto a singular set as  $t \rightarrow \infty$ .

## Acknowledgements

We warmly thank F. Bagnoli for useful discussions and help in numerical calculations. This work has been financially supported by The University of Florence, INFN, MIUR-COFIN03 contract *Order and chaos in nonlinear extended systems* and the FIRB n. RBNE01CW3M\_01 project on synchronization.



## References

- [1] H. Koyama and T. Konishi, Phys. Lett. A **279**, 226 (2001).
- [2] V. Latora, A. Rapisarda, C. Tsallis, Phys. Rev. E **64**, 056134 (2001) and Physica A **305**, 129 (2002).
- [3] K. Falconer, *Fractal geometry: mathematical foundations and applications*, Wiley (1990).
- [4] F. Hohl and M.R. Feix, Astroph. J., **147**, 1164 (1967).
- [5] M. Antoni and S. Ruffo, Phys. Rev. E **52**, 2361 (1995).
- [6] H. Spohn, *Large Scale Dynamics of Interacting Particles*, Springer (1991).
- [7] B.V. Chirikov, Phys. Rep.,**52**, 263 (1979).
- [8] T. Dauxois, V. Latora, A. Rapisarda, S. Ruffo, A. Torcini, *The Hamiltonian Mean Field Model: from Dynamics to Statistical Mechanics and back*, in *Dynamics and thermodynamics of systems with long range interactions*, T. Dauxois et al. Eds., Lecture Notes in Physics **602**, Springer (2002).
- [9] Y.Y. Yamaguchi, J. Barré, F. Bouchet, T. Dauxois and S. Ruffo, Physica A, **337**, 36 (2004).
- [10] J.M. Ottino, *The kinematics of mixing: stretching, chaos and transport*, Cambridge University Press (1989).
- [11] G. Benettin, D. Casati, L. Galgani and A. Giorgilli, Phys. Lett. A, **118**, 325 (1986).
- [12] T. Tatekawa and K. Maeda, Astroph. J. **547**, 531 (2001).
- [13] B.N. Miller and J.L. Rouet, Phys. Rev. E **65**, 056121 (2001).
- [14] T. Tel et al., Chaos, **10**, 89 (2000).
- [15] E. Ott and T.M. Antonsen Jr., Phys. Rev. A, **39**, 3660 (1989).